Frontiers in Heat and Mass Transfer (FHMT), 12, 23 (2019)
DOI: 10.5098/hmt.12.23

Global Digital Central
ISSN: 2151-8629

Frontiers in Heat and Mass Transfer

Available at www.ThermalFluidsCentral.org

A STUDY OF MAGNETIC EFFECT ON FLOW BETWEEN TWO PLATES WITH SUCTION OR INJECTION WITH SPECIAL REFERENCE TO CASSON FLUID

V. S. Sampath Kumar and N. P. Pai†

Manipal Institute of Technology, Manipal Academy of Higher Education, Manipal, Karnataka, 576104, India

ABSTRACT

The present paper encorporates the effet of magnetic field on the incompressible Casson fluid flow between two parallel infinite rectangular plates approaching towards or away from each other with suction or injection at the porous plates. Using similarity transformations the governing Navier-Stokes equations are reduced to a nonlinear ordinary differential equation. Semi-analytical solution is obtained based on the Homotopy perturbation method. Further, the solution is compared with the classical finite difference method separately. The effect of magnetic field on velocity, skin friction and pressure is analysed on flow between two plates with suction or injection, where two plates moving towards or away from each other.

Keywords: *Porous plates; Casson fluid; Incompressible flow; Homotopy Perturbation method; Finite Difference Method*

1. INTRODUCTION

The rapid advancements in technology and industries, the flow between porous structures have acquired the attention of numerous researchers in recent times due to their applications in the field of medicine and industry. Specifically, the flow of blood through arteries, pumping of heart, polymer industry process, injection modeling, compression, power transmission and lubrication technology can be grasped by the basic fluid flow between porous structures. Due to the complex rheological behavior of many classical and biological liquids, it is difficult to understand the various physiological behaviors by taking the Newtonian fluids. Thus, their exists several non-Newtonian fluid models to encorporates these effects (Sankad and Patil (2018); Rajashekhar *et al.* (2018); Boulahia *et al.* (2018)). In recent years study, the Casson fluid flow between two plates grasp the attention of researchers due to its practical applications. In 1959 N. Casson developed this model in the rheology of dispersed system. Fung and his associates in 1981 used Casson model to study the behavior of blood. Milnor, Bate and Merrill concluded that the blood flow through tubes is best described by Casson equation.

The basic work and formulation of squeezing flows are firstly has done by Stefan in 1874. After that, many researchers (Grimm (1976), Kuzma (1966), Tichy and Winer (1970), Jackson (1963)) contributed towards better understanding of this phenomenon. Reynolds in 1986 (Reynolds (1886)) analyse the squeezing flow between elliptic plates, Archibald Archibald (1956) extended this work for rectangular plates. In the 19th century, many researchers studied the same type of problems by reducing the Navier-Stokes equation to nonlinear ordinary differential equation or set of nonlinear differential equations through similarity transformation. In 1999 E. A. Hamza Hamza (1999) studied the suction and injection effects on a similar flow between parallel plates. Siddiqui, et al.(Domairry and Aziz (2009), Abdul *et al.* (2008)) analysed the two dimensional MHD squeezing flow between parallel plates using the homotopy perturbation method. T. Hayat and his co-workers (Hayat *et al.* (2008, 2010, 2011, 2015)) analyse the fluid flow phenomenon under different conditions and situations. Recently, many researchers contributed their knowledge to study MHD problems (Sheikh *et al.* (2015); Imran *et al.* (2017); Umar *et al.* (2016, 2014); Sobamowo and Akinshilo (2018); Sufian *et al.* (2012)). The detailed study of nano fluids under different conditions and effects is well established by Abderrahim Wakif and his associates(Abderrahim *et al.* (2017a,b, 2018c,b, 2019, 2018a); Saleem *et al.* (2019)).

This type of study mainly involves two sections, first one mathematical formulation, the second solution of the problem. Most of this kind of problems is highly nonlinear, solving these really challenges to the research community, many authors solved them using numerical and semi-numerical methods (Sachdev *et al.* (2000); Shijun (2011)). The Homotopy perturbation method is one of the simplest methods to handle these type of problems(Ji-Huan (2008); Sumit *et al.* (2013, 2006); Babolian *et al.* (2009); Bujurke *et al.* (1995b,a); Sampath and Pai (2019)). The advantage of HPM is a single computer program run yields the solution for a large range of the expansion quantity rather than a solution for a single value. In addition the method reveals the analytical structure of the solution function. For simple geometry the method proposed her, provides accurate results and has advantages over pure numerical methods like finite difference. In numerical methods a separate scheme is to be devolved for calculating derived quantities. Such difficulties are not there in HPM.

† *Corresponding author. Email: nppaimit@yahoo.co.in*

Global Digital Central
ISSN: 2151-8629

2. MATHEMATICAL FORMULATIONS

We consider the two dimensional incompressible Casson fluid flow between two parallel infinite rectangular plates which are spaced a distance $a(t)$ apart, where t denotes time. We specify the plates by $y = 0$ and $y = a(t), a(0) = a_0$, and the upper plate is moving with velocity $a'(t)$ towards (or away from) the lower porous plate which is fixed.

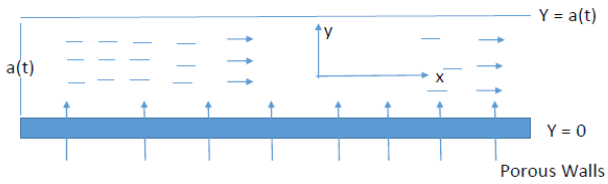

Fig. 1 Geometry of the problem

The equation of Casson fluid is defined as

$$\tau_{ij} = \left[\mu_B + \left(\frac{p_y}{\sqrt{2\pi}}\right)^{\frac{1}{n}}\right]^n 2e_{ij}, \tag{1}$$

where p_y is the yield stress, μ_B is the Casson viscosity and $\pi = e_{ij}e_{ij}$, where e_{ij} is the (i, j) components of the deformation rate. The governing equations are

$$\frac{\partial u}{\partial x} + \frac{\partial v}{\partial y} = 0, \tag{2}$$

where u and v are velocity components along x and y axis respectively. The equations governing the flow in cartesian coordinates are

$$\frac{\partial u}{\partial t} + u\frac{\partial u}{\partial x} + v\frac{\partial u}{\partial y} = -\frac{1}{\rho}\frac{\partial p}{\partial x} + \nu(1+\frac{1}{\gamma})(2\frac{\partial^2 u}{\partial x^2} + \frac{\partial^2 u}{\partial y^2} + \frac{\partial^2 v}{\partial x \partial y}) - \frac{\sigma\beta^2}{\rho}u, \tag{3}$$

$$\frac{\partial v}{\partial t} + u\frac{\partial v}{\partial x} + v\frac{\partial v}{\partial y} = -\frac{1}{\rho}\frac{\partial p}{\partial y} + \nu(1+\frac{1}{\gamma})(\frac{\partial^2 v}{\partial x^2} + 2\frac{\partial^2 v}{\partial y^2} + \frac{\partial^2 u}{\partial x \partial y}), \tag{4}$$

and

$$\frac{\partial T}{\partial t} + u\frac{\partial T}{\partial x} + v\frac{\partial T}{\partial y} = \frac{k}{\rho C_p}(\frac{\partial^2 T}{\partial x^2} + \frac{\partial^2 T}{\partial y^2}) + \frac{\nu}{C_p}(1+\frac{1}{\gamma})\left[2(\frac{\partial^2 u}{\partial x^2})^2 + 2(\frac{\partial^2 v}{\partial y^2})^2 + (\frac{\partial^2 v}{\partial x^2} + \frac{\partial^2 u}{\partial y^2})^2\right] \tag{5}$$

Where $\gamma = \mu_B\sqrt{2\pi}/p_y$ and ν is the kinematic viscosity of the fluid. T is the temperature, C_p is the specific heat and k is the thermal conductivity. Viscosity of the fluid is taken as constant and it does not depend on temperature.
The boundary conditions are given by

$$u(x, y, t) = 0, \quad v(x, y, t) = a'(t), \quad T = T_H \quad \text{at} \quad y = a(t), \tag{6}$$

$$u(x, y, t) = 0, \quad v(x, y, t) = Aa'(t), \quad \frac{\partial T}{\partial y} = 0, \quad \text{at} \quad y = 0. \tag{7}$$

Where A is a constant parameter such that $A > 0$ corresponds to suction and $A < 0$ corresponds to injection.
Using the transformation

$$u = \frac{C-x}{a(t)}a'(t)f'(\eta), \qquad v = a'(t)f(\eta). \qquad \theta = \frac{T}{T_H} \tag{8}$$

Where $\eta = \frac{y}{a(t)}$ and C is a constant.
The equation of motion is satisfied and the equation of motion takes the form

$$\frac{\partial p}{\partial x}\frac{1}{C-x} = \frac{\rho a'^2}{a^2}\{\frac{1+\frac{1}{\gamma}}{R}f''' - Qf' + \eta f'' + f' + f'^2 - ff''\} + \sigma\beta^2\frac{a'}{a}f' = P_1(\eta, t), \tag{9}$$

$$\frac{\partial p}{\partial \eta} = \rho a'^2\{\frac{(1+\frac{1}{\gamma})}{R}f'' - ff' + \eta f' - Qf\} = P_2(\eta, t). \tag{10}$$

Where

$$R = \frac{aa'}{\nu}, \qquad Q = \frac{aa''}{a'^2}. \tag{11}$$

The equation for the axial pressure gradient $\frac{\partial p}{\partial \eta}$ gives

$$\frac{\partial^2 p}{\partial x \partial \eta} = 0.$$

This shows that

$$\frac{1}{C-x}\frac{\partial p}{\partial x} = P_1(t)$$

. Differentiating (9) with respect to η gives

$$(1+\frac{1}{\gamma})f^{iv} = R(ff''' - f'f'' - \eta f''' - 2f'' + Qf'') - M^2 f''. \tag{12}$$

For a similarity solution to exist, R and Q must be constant, since $a' = \frac{da(t)}{dt}$, the first equation (11) can be integrated to give

$$a(t) = (2\gamma Rt + a_0^2)^{\frac{1}{2}}. \tag{13}$$

When $R > 0$ the upper plate moves away from the lower plate and when $R < 0$, it moves towards it, and squeezing flow exists with similar velocity profiles as long as $a(t) > 0$.
From (11) and (13) it follows that $Q = -1$ and hence equations take the form

$$(1+\frac{1}{\gamma})f^{iv} = R(ff''' - f'f'' - \eta f''' - 3f'') - M^2 f''. \tag{14}$$

and

$$\theta'' + P_r R(f\theta' - \eta\theta') + P_r E_c(1+\frac{1}{\gamma})(f''^2 + 4\delta^2 f'^2) = 0 \tag{15}$$

The boundary conditions are

$$f(1) = 1, \quad f'(1) = 0, \quad f(0) = A, \quad f'(0) = 0, \theta(1) = 1, \theta'(0) = 0 \tag{16}$$

Where P_r is Prandtl number, E_c Eckert number and δ is small number.
We solve equations (14) to (16) to see the effects of R and A on the velocity profiles, the skin friction and the pressure distribution for different values of Casson parameter.

2.1. The skin friction

The skin friction at the wall is represented by

$$S = \mu(1+\frac{1}{\gamma})(\frac{\partial u}{\partial y})_{y=a(t)}, \tag{17}$$

where μ is the coefficient of viscosity.
or

$$S^* = (1+\frac{1}{\gamma})f''(1),$$

where

$$S^* = \frac{a^2}{\mu a'(C-x)}S.$$

Global Digital Central
ISSN: 2151-8629

2.2. The pressure distribution

The fluid pressure is obtained by partial integrating (9 and 10). The pressure along x- direction

$$p(x,t)-p_0=-\frac{-\rho a'^2 L}{2a^2}\left[(c-x)^2-(c-l)^2,\right] \tag{18}$$

where

$$L=\frac{1+\frac{1}{\gamma}}{R}f'''(0)-Af''(0), \tag{19}$$

l is the length of the plate from the origin and p_0 is the atmospheric pressure at $x=l$. This can be written in dimensionless form as

$$p^x=L,$$

where

$$p^x=-\frac{2a^2[p(x,t)-p_0]}{\rho a'^2[(c-x)^2-(c-l)^2]}.$$

The η distribution of pressure is equal to

$$p(\eta,t)-p_e=\rho a'^2(\eta f+\frac{1}{2}(A^2-f^2)+\frac{(1+\frac{1}{\gamma})}{R}f'),$$

where p_e is the pressure at $\eta=0$ or

$$p^\eta=\eta f+\frac{1}{2}(A^2-f^2)+\frac{1+\frac{1}{\gamma}}{R}f',$$

where

$$p^\eta=\frac{p(\eta,t)-p_e}{\rho a'^2}.$$

3. METHOD OF SOLUTION

We adopt two methods to solve the considered problems.
Method-I: Homotopy Perturbation Solution:
To describe the HPM solution for the system of non-linear differential equations, we consider

$$D_1[f(\eta)]-f_1(\eta)=0 \tag{20}$$

$$D_2[\theta(\eta)]-f_2(\eta)=0 \tag{21}$$

where D_1 and D_2 denotes the operator, $f(\eta)$ and $\theta(\eta)$ are unknown functions, η denote the independent variable and f_1, f_2 are known functions. D_1 and D_2 can be written as

$$D_1=L1+N1$$

$$D_2=L2+N2$$

where $L1$ and $L2$ are simple linear part, $N1$ and $N2$ are remaining part of the equations (20, 21) respectively. The proper selection of $L1$, $L2$, $N1$, and $N2$ form the governing equations one can get the homotopy equation for (20 and 21) as follows

$$\begin{aligned}H1(\Phi1(\eta,q;q))=(1-q)\big[L1(\Phi1,q)-L1(v_0(\eta))\big]\\+q\big[D1(\Phi1,q)-f_1(\eta)\big]=0\end{aligned} \tag{22}$$

$$\begin{aligned}H2(\Phi2(\eta,q;q))=(1-q)\big[L2(\Phi1,q)-L2(v_0(\eta))\big]\\+q\big[D2(\Phi2,q)-f_2(\eta)\big]=0\end{aligned} \tag{23}$$

where $v_0(\eta)$ is the initial guess to the (20,21).
We assume the solution of (22) and (23) as follows

$$\Phi1(\eta,q)=\sum_{n=0}^{\infty}q^n f_n(\eta) \tag{24}$$

$$\Phi2(\eta,q)=\sum_{n=0}^{\infty}q^n \theta_n(\eta) \tag{25}$$

The solution to the considered problems is (24 and 25) at $q=1$.
Using the above scheme for solving the equations, zeroth and first order solutions are obtained as follows.

$$u_0=A+3\eta^2-3A\eta^2-2\eta^3+2A\eta^3$$

$$\begin{aligned}u_1=\frac{1}{140(1+\gamma)}\big[-7M\gamma\eta^2+7M^2A\gamma\eta^2-25R\gamma\eta^2\\-13AR\gamma\eta^2+38A^2R\gamma\eta^2+28M^2\gamma\eta^3-28M^2A\gamma\eta^3+96R\gamma\eta^3\\-10AR\gamma\eta^3-86A^2R\gamma\eta^3-35M^2\gamma\eta^4\\+35M^2A\gamma\eta^4-105R\gamma\eta^4+35AR\gamma\eta^4+70A^2R\gamma\eta^4\\+14M^2\gamma\eta^5-14M^2A\gamma\eta^5+14R\gamma\eta^5\\+28AR\gamma\eta^5-42A^2R\gamma\eta^5\\+28R\gamma\eta^5-56AR\gamma^6+28A^2R\gamma\eta^6-8R\gamma\eta^6\\+16AR\gamma\eta^7-8A^2R\gamma\eta^7\big]\end{aligned}$$

$$\begin{aligned}\theta_0=\frac{1}{5\gamma}\Big[5\gamma-6(-1+A)^2E_cP_r(1+\gamma)(-1+\eta)\Big\{5(1+\eta-2\eta^2+2\eta^3)\\+2\delta^2(1+\eta+\eta^2+\eta^3-4\eta^4+2\eta^5)\Big\}\Big]\end{aligned}$$

$$\begin{aligned}\theta_1=\frac{1}{525\gamma}(-1+A)^2E_cP_r(-1+\eta)\Big\{3P_rR(1+\gamma)(-5(2+2\eta+2\eta^2\\+2\eta^3-103\eta^4\\+212\eta^5-180\eta^6+60\eta^7)+\delta^2(3+3\eta+3\eta^2+3\eta^3\\+3\eta^4+3\eta^5+283\eta^6-617\eta^7+448\eta^8-112\eta^9)\\+A(15(17+17\eta+17\eta^2\\-53\eta^3+17\eta^4+52\eta^5-60\eta^6+20\eta^7)+\delta^2(47+47\eta^2\\+47\eta^3+47\eta^4-373\eta^5+47\eta^6+527\eta^7\\-448\eta^8+112\eta^9)))+\gamma(3M^2(35\eta^2(-3+11\eta-16\eta^2+8\eta^3)\\+\delta^2(-1-\eta-\eta^2-\eta^3-71\eta^4+223\eta^5\\-225\eta^6+75\eta^7))-R(15\eta^2(75-263\eta\\+340\eta^2-80\eta^3-108\eta^3-108\eta^4+36\eta^5)\\+\delta^2(11+11\eta+11\eta^2+11\eta^3+761\eta^4\\-2281\eta^5+1976\eta^6-133\eta^7-448\eta^8+112\eta^9))\\+AR(30(7+7\eta-50\eta^2\\+117\eta^3-117\eta^4+72\eta^5-54\eta^6\\+18\eta^7)+\delta^2(29+29\eta+29\eta^2+29\eta^3-1111\eta^4\\+1895\eta^5-1333\eta^6+767\eta^7-448\eta^8+112\eta^9))\Big\}\end{aligned}$$

Method-II: Finite Difference Solution:
The equation mentioned above (14) to (16) is solved numerically by FDM to confirm the results obtained by us. Using standard finite difference method, i.e. stepping from η_{j-1} to η_j, a Crank-Nicolson's scheme is used. This tridiagonal system is easily solved to update the values on each grid point. Calculations were performed by dividing the interval into 10^4 sub intervals to find the associated parameters. These systems of equations are solved using Mathematica.

4. RESULTS AND DISCUSSION

In the present study, we have analysed the effect of magnetic field, suction or injection on fluid flow between two parallel plates either the plates moving towards or away from each other. We used HPM to analyse $f(\eta)$, $f'(\eta)$ and p^η for different values of the parameters and presented the results from Fig. 2 to Fig. 20, for this we consider 20 terms in the

series by writing a mathematica code. The Values of the skin friction and p^x also analysed through HPM and are compared with FDM and results are presented (Table 1 to 5). We split the result and discussion into two parts.

a) Injection case ($A < 0$): Fig. 2 shows the effect of R on velocity of the fluid. It is observed that, when the upper plate moving away from the lower plate, the velocity of fluid is increased in the half plane ($0 \leq \eta \leq 0.5$) and has opposite behavior is observed in $0.5 \leq \eta \leq 1$. When the plates moving towards each other, the velocity decreases in $0 \leq \eta \leq 0.5$ and increases in $0.5 \leq \eta \leq 1$. The most common observation in this case is, the peakness of velocity increases, when the plates moving away from each other and it is less, when the plates are moving towards each other. This is due to the non-Newtonian characteristic of the fluid. From Fig. 3 to 5, it is clear that in the presence of magnetic effect, the fluid flow is smoother. The velocity increases with the effect of magnet in $0 \leq \eta \leq 0.3$ and $0.7 \leq \eta \leq 1$. The opposite behavior is observed in $0.4 \leq \eta \leq 0.7$.

b) Suction Case($A > 0$): The velocity of the fluid, when the plates approaching or receding each other are given in Fig.6. The velocity of fluid decreases in $0 \leq \eta \leq 0.5$ and increases in $0.5 \leq \eta \leq 1$, when the plates moving away from each other. The reverse effect is observed during the plates moving towards each other. Fig. 7 to 11 show the effect of M when $R = -10, 10, -0.01, 0.01$. Here it is observed that, fluid flow is smoother and there is no disturbance in the flow due to magnetic effects. Fig. 12 to 15 describe the effect of Casson fluid parameter γ, under different conditions. It is evident that the value of the γ increases, the non-Newtonian characteristics increases and the flow become smoother. Fig. 16 and 17 represents the axial pressure with suction and injection respectively.

The skin friction under different conditions are calculated through FDM and HPM (Table 1 and 2). From these tables we observe that the absolute value of skin friction decreases as we increase the effect of M in both suction and injection cases when plates moving away or towards each other. The absolute value of the skin friction increases when the plates moving towards each other and reverse effect is observed during the plates moving away from each other. Tables 3 and 4 show the effect of dimensional x pressure under different conditions. Further the absolute value of the pressure increases when plates moving towards each other.

Fig. 18 to 20 show the temperature distribution with respect to various parameters. It is observed that as E_c increases temperature also increases, whereas with increase in γ temperature decreases. Also as δ increases, temperature decreases. Further, it is understood that the results are same for suction or injection. The variation of $\theta'(1)$ for different values of γ and R for fixed values of P_r, E_c, δ and M listed in table 5.

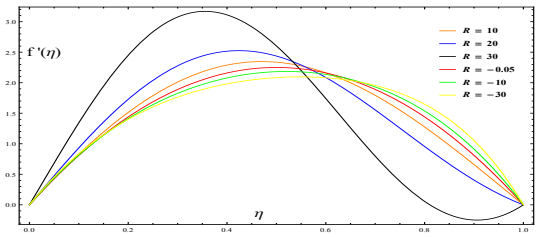

Fig. 2 Variation of the dimensionless function $f'(\eta)$ with R, $\gamma = 0.3$, $A = -0.5$,$M = 0.3$

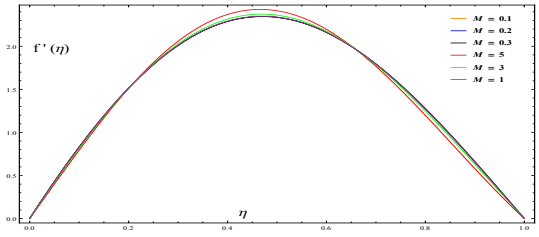

Fig. 3 Variation of the dimensionless function $f'(\eta)$ with M, $\gamma = 0.3$, $A = -0.5$, $R = 10$

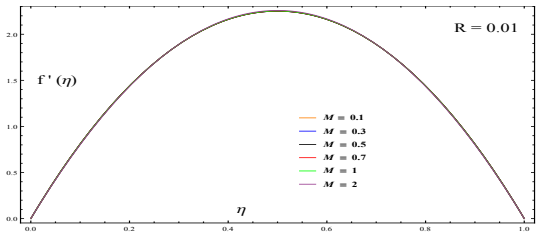

Fig. 4 Variation of the dimensionless function $f'(\eta)$ with M, $R = 0.01$, $A = -0.5$, $\gamma = 0.3$

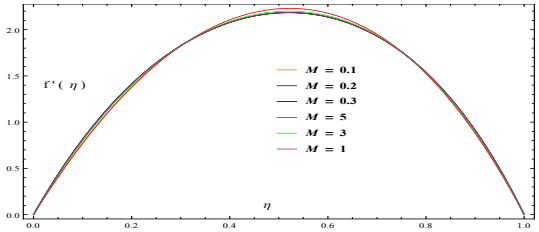

Fig. 5 Variation of the dimensionless function $f'(\eta)$ with M, $\gamma = 0.3$, $A = -0.5$, $R = -10$

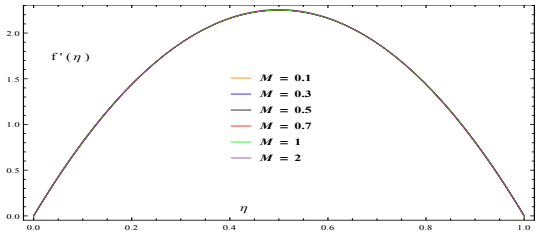

Fig. 6 Variation of the dimensionless function $f'\eta$ with M, $\gamma = 0.3$, $A = -0.5$, $R = -0.01$

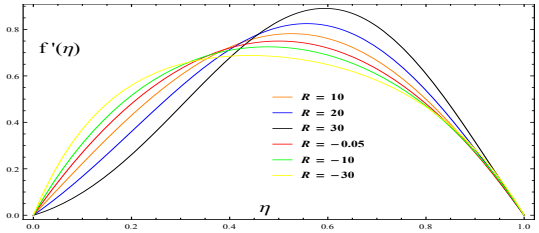

Fig. 7 Variation of the dimensionless function $f'(\eta)$ with R, $\gamma = 0.3$, $A = 0.5$, $M = 0.3$

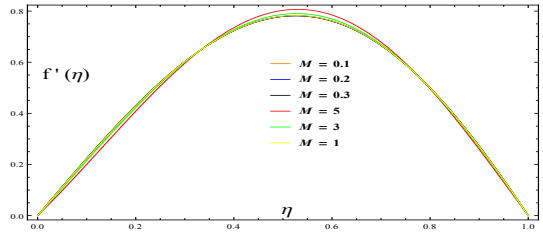

Fig. 8 Variation of the dimensionless function $f'(\eta)$ with M, $\gamma = 0.3$, $A = 0.5$, $R = 10$

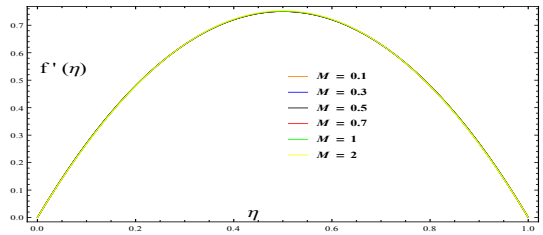

Fig. 9 Variation of the dimensionless function $f'(\eta)$ with M, $\gamma = 0.3$, $A = 0.5$, $R = 0.01$

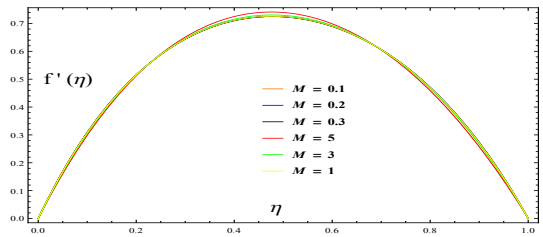

Fig. 10 Variation of the dimensionless function $f'(\eta)$ with M, $\gamma = 0.3$, $A = 0.5$, $R = -10$

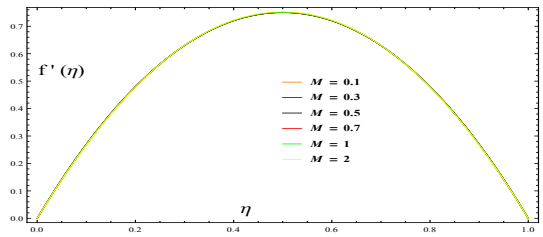

Fig. 11 Variation of the dimensionless function $f'(\eta)$ with M, $\gamma = 0.3$, $A = 0.5$, $R = -0.01$

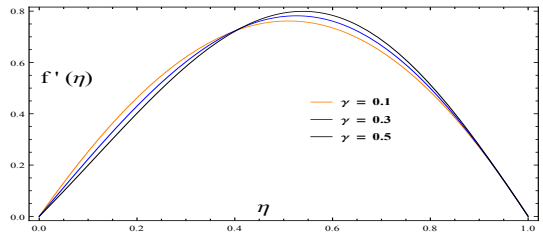

Fig. 12 Variation of the dimensionless function $f'(\eta)$ with γ, $M = 0.3$, $A = 0.5$, $R = 10$

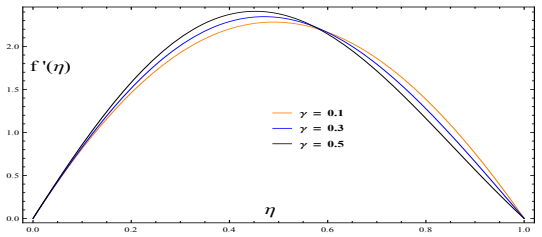

Fig. 13 Variation of the dimensionless function $f'(\eta)$ with γ, $M = 0.3$, $A = -0.5$, $R = 10$

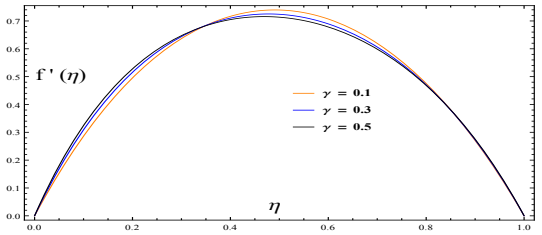

Fig. 14 Variation of the dimensionless function $f'(\eta)$ with γ, $M = 0.3$, $A = 0.5$, $R = -10$

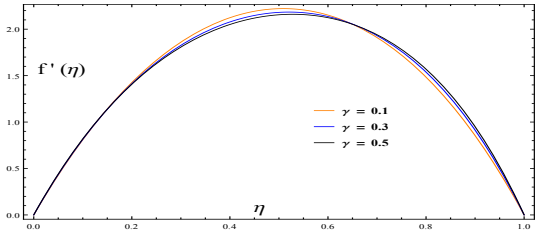

Fig. 15 Variation of the dimensionless function $f'(\eta)$ with γ, $M = 0.3$, $A = -0.5$, $R = -10$

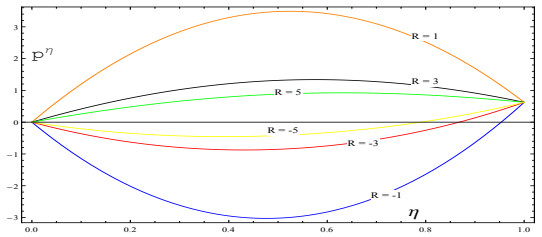

Fig. 16 Variation of the dimensionless axial pressure P^{η} with R, when$A = 0.5$,$\gamma = 0.3$, $M = 0.3$

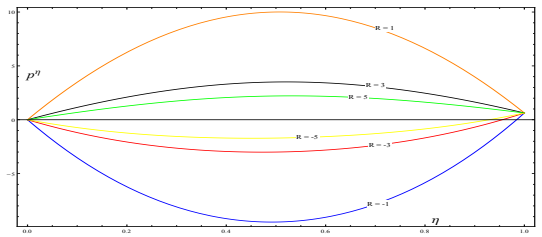

Fig. 17 Variation of the dimensionless axial pressure P^{η} with R, when$A = -0.5$,$\gamma = 0.3$, $M = 0.3$

Table 1 Values of skin friction coefficient when $\gamma = 0.1$

		$A = 0.5$		$A = -0.5$	
R	M	HPM	FDM	HPM	FDM
1	0.1	-32.9356	-32.9310	-98.1154	-98.0961
5		-32.6886	-32.6796	-94.4890	-98.4694
10		-32.4012	-32.3935	-89.7258	-89.7083
15		-32.1410	-32.1343	-84.6728	-84.6528
20		-31.9123	-31.9058	-79.2864	-79.2656
25		-31.7200	-31.7157	-73.5124	-73.4932
30		-31.5696	-31.5646	-67.2824	-67.2637
-1		-33.0642	-33.0575	-99.8727	-99.8523
-5		-33.3304	-33.0575	-103.2840	-103.2630
-10		-33.6785	-33.6731	-107.3700	-107.3510
-15		-34.0411	-34.0349	-111.2790	-111.2580
-20		-34.4159	-34.4093	-115.0280	-115.0060
-25		-34.8009	-34.7951	-118.6330	-118.6090
-30		-35.1944	-35.1887	-122.1070	-122.0850
1	0.3	-32.9316	-32.9263	-98.1033	-98.0849
5		-32.6846	-32.6787	-94.4763	-94.4564
10		-32.3972	-32.3899	-89.7123	-89.6927
15		-32.1370	-32.1289	-84.6584	-84.6404
20		-31.9084	-31.9027	-79.2710	-79.2517
25		-31.7162	-31.7125	-73.4957	-73.4774
30		-31.5659	-31.5583	-67.2643	-67.2472
-1		-33.0602	-33.0527	-99.8608	-99.8396
-5		-33.3264	-33.3217	-103.2730	-103.2520
-10		-33.6745	-33.6688	-107.3600	-107.3390
-15		-34.0371	-34.0308	-111.2690	-111.2470
-20		-34.4119	-34.4090	-115.0180	-114.9970
-25		-34.7970	-34.7912	-118.6230	-118.6000
-30		-35.1905	-35.1834	-122.0980	-122.0750
1	0.5	-32.9236	-32.9175	-98.0790	-98.0622
5		-32.6767	-32.6696	-94.4510	-94.4326
10		-32.3893	-32.3805	-89.6854	-89.6669
15		-32.1292	-32.1213	-84.6297	-84.6120
20		-31.9007	-31.8909	-79.2401	-79.2240
25		-31.7086	-31.7029	-73.4624	-73.4445
30		-31.5585	-31.5538	-67.2280	-67.2091
-1		-33.0522	-33.0455	-99.8370	-99.8159
-5		-33.3184	-33.3123	-103.2500	-103.2300
-10		-33.6665	-33.6577	-107.3380	-107.3180
-15		-34.0291	-34.0209	-111.2480	-111.2260
-20		-34.4040	-34.3970	-114.9980	-114.9750
-25		-34.7891	-34.7806	-118.6040	-118.5830
-30		-35.1827	-35.1772	-122.0790	-122.0560

Table 2 Values of skin friction coefficient when $\gamma = 0.3$

		$A = 0.5$		$A = -0.5$	
R	M	HPM	FDM	HPM	FDM
1	0.1	-12.9363	-12.9334	-38.1083	-38.1007
5		-12.7072	-12.7037	-34.2888	-34.2818
10		-12.4903	-12.4871	-28.7761	-28.7694
15		-12.3818	-12.3803	-22.0669	-22.0599
20		-12.4263	-12.4228	-13.3769	-13.3689
25		-12.6848	-12.6836	-0.7245	-0.7175
30		-13.2404	-13.2403	22.3176	22.0709
-1		-13.0648	-13.0618	-39.8660	-39.8582
-5		-13.3432	-13.3405	-43.1340	-43.1255
-10		-13.7210	-13.7191	-46.8404	-46.8318
-15		-14.1201	-14.1171	-50.2154	-50.2061
-20		-14.5317	-14.5286	-53.3271	-53.3177
-25		-14.9493	-14.9461	-56.2249	-56.2152
-30		-15.3685	-15.3658	-58.9777	-58.9346
1	0.3	-12.9323	-12.9295	-38.0960	-38.0884
5		-12.7032	-12.7013	-34.2749	-34.2681
10		-12.4865	-12.4840	-28.7594	-28.7521
15		-12.3783	-12.3770	-22.0457	-22.0399
20		-12.4234	-12.4220	-13.3477	-13.3413
25		-12.6828	-12.6819	-0.6775	-0.67114
30		-13.2397	-13.2392	22.4160	22.1676
-1		-13.0608	-13.0578	-39.8543	-39.8465
-5		-13.3393	-13.3369	-43.1234	-43.1151
-10		-13.7170	-13.7152	-46.8309	-46.8221
-15		-14.1163	-14.1135	-50.2066	-50.1976
-20		-14.5279	-14.5252	-53.3190	-53.3096
-25		-14.9457	-14.9434	-56.2173	-56.2067
-30		-15.3648	-15,3623	-58.9702	-58.9277
1	0.5	-12.9243	-12.9223	-38.0713	-38.0629
5		-12.6953	-12.6926	-34.2470	-34.2397
10		-12.4789	-12.4751	-28.7258	-28.7189
15		-12.3713	-12.3705	-22.0031	-22.9959
20		-12.4175	-12.4160	-13.2892	-13.2825
25		-12.6787	-12.6776	-0.5832	-0.5756
30		-13.2385	-13.2378	22.6135	22.3546
-1		-13.0528	-13.0502	-39.8309	-39.8229
-5		-13.3313	-13.3279	-43.1021	-43.0938
-10		-13.7092	-13.7069	-46.8117	-46.8023
-15		-14.1086	-14.1061	-50.1891	-50.1801
-20		-14.5204	-14.5182	-53.3027	-53.2930
-25		-14.9384	-14.9353	-56.2021	-56.1918
-30		-15.3577	-15.3548	-58.9548	-58.9133

Table 3 Values of the dimensional x pressure p^x when $\gamma = 0.1$

		$A = 0.5$		$A = -0.5$	
R	M	HPM	FDM	HPM	FDM
1	0.1	-64.5151	-64.4934	-190.068	-190.0230
5		-11.7185	-11.719	-31.6523	-31.6491
10		-5.1174	-5.1186	-11.8151	-11.8179
15		-2.9159	-5.1186	-5.1743	-5.1795
20		-1.8144	-1.8155	-1.8304	-1.8357
25		-1.1528	-1.1538	0.1970	0.1913
30		-0.7113	-0.7124	1.5688	1.5624
-1		67.4722	67.4455	205.882	205.8080
-5		14.6756	14.6700	47.4685	47.4475
-10		8.0745	8.0695	27.637	27.6225
-15		5.8729	5.8685	21.0059	20.9930
-20		4.7712	4.7668	17.6759	17.6643
-25		4.1095	4.1054	15.6672	15.6561
-30		3.6677	3.6637	14.3197	14.3089
1	0.3	-64.4670	-64.4462	-189.9230	-189.8130
5		-11.7089	-11.7071	-31.6232	-31.6192
10		-5.1126	-5.1139	-11.8004	-11.8025
15		-2.9127	-2.9138	-5.1644	-5.1686
20		-1.8120	-1.8131	-1.8228	-1.8286
25		-1.1509	-1.1518	0.2031	0.1971
30		-0.7096	-0.7111	1.5739	1.5674
-1		67.4243	67.4048	205.738	205.6730
-5		14.6661	14.6575	47.4400	47.4187
-10		8.0697	8.0650	27.6228	27.6081
-15		5.8697	5.8654	20.9965	20.9839
-20		4.7689	4.7644	17.6689	17.6572
-25		4.1076	4.1036	15.6616	15.6506
-30		3.6661	3.6621	14.3151	14.3042
1	0.5	-64.371	-64.3520	-189.6350	-189.5730
5		-11.6896	-11.6874	-31.5651	-31.5618
10		-5.1029	-5.1033	-11.7710	-11.7731
15		-2.9062	-2.9071	-5.1446	-5.1487
20		-1.8071	-1.8086	-1.8078	-1.8134
25		-1.1469	-1.1484	0.2153	0.2094
30		-0.7063	-0.7087	1.5842	1.5779
-1		67.3283	67.3103	205.4510	205.388
-5		14.6470	14.6412	47.3829	47.3622
-10		8.0602	8.0559	27.5945	27.5801
-15		5.8634	5.8593	20.9777	20.9655
-20		4.7641	4.7601	17.6550	17.6435
-25		4.1038	4.1000	15.6505	15.6394
-30		3.6631	3.6591	14.3059	14.2949

Table 4 Values of the dimensional x pressure p^x when $\gamma = 0.3$

		$A = 0.5$		$A = -0.5$	
R	M	HPM	FDM	HPM	FDM
1	0.1	-24.5145	-24.5112	-70.0563	-70.0419
5		-3.7159	-3.7175	-7.5912	-7.5953
10		-1.1123	-1.1136	0.3220	0.3162
15		-0.2418	-0.2428	3.0662	3.0593
20		0.1958	0.1947	4.5814	4.5737
25		0.4612	0.4604	5.8065	5.7976
30		0.6428	0.6424	7.7649	7.7077
-1		27.4717	27.4644	85.8712	85.8378
-5		6.6729	6.6689	23.4180	23.4048
-10		4.0690	4.0648	15.5440	15.5326
-15		3.1980	3.1940	12.8770	12.8665
-20		2.7602	2.7562	11.5169	11.5066
-25		2.4959	2.4916	10.6827	10.6726
-30		2.3183	2.3138	10.1130	10.1037
1	0.3	-24.4664	-24.4613	-69.9116	-69.8960
5		-3.7062	-3.7066	-7.5617	-7.5655
10		-1.1074	-1.1088	0.3372	0.3313
15		-0.2385	-0.2397	3.0768	3.0699
20		0.1983	0.1973	4.5899	4.5822
25		0.4632	0.4624	5.8147	5.8058
30		0.6445	0.6440	7.7781	7.7203
-1		27.4238	27.4135	85.7278	85.6941
-5		6.6634	6.6590	23.3898	23.3764
-10		4.0643	4.0601	15.5301	15.5189
-15		3.1949	3.1907	12.8679	12.8574
-20		2.7579	2.7538	11.5102	11.4996
-25		2.4940	2.4898	10.6774	10.6674
-30		2.3167	2.3123	10.1086	10.0992
1	0.5	-24.3702	-24.3649	-69.6222	-69.6109
5		-3.6868	-3.6879	-7.5026	-7.5062
10		-1.0976	-1.0991	0.3677	0.3613
15		-0.2319	-0.2329	3.0980	3.0910
20		0.2033	0.2023	4.6070	4.5992
25		0.4673	0.4666	5.8313	5.8223
30		0.6479	0.6475	7.8046	7.7452
-1		27.3280	27.3165	85.4411	85.4107
-5		6.6444	6.6403	23.3333	23.3201
-10		4.0549	4.0508	15.5024	15.4914
-15		3.1887	3.1847	12.8497	12.8393
-20		2.7533	2.7492	11.4967	11.4865
-25		2.4904	2.4863	10.6667	10.6566
-30		2.3137	2.3093	10.0998	10.0904

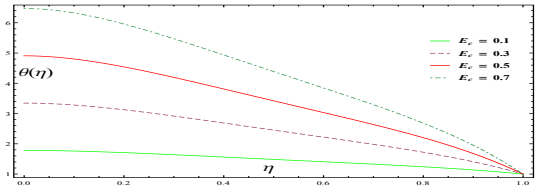

Fig. 18 Variation of the $\theta(\eta)$ with E_c, when$R = 1, P_r = 0.5, M = 0.3, \delta = 0.1, \gamma = 0.1, A = 0.5$

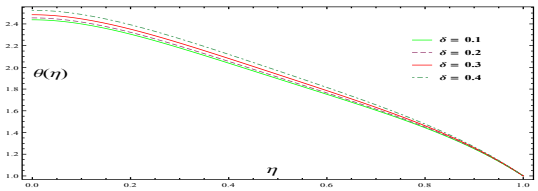

Fig. 19 Variation of the $\theta(\eta)$ with δ, when$R = 1, P_r = 0.3, M = 0.3, \gamma = 0.1, A = 0.5, E_c = 0.3$

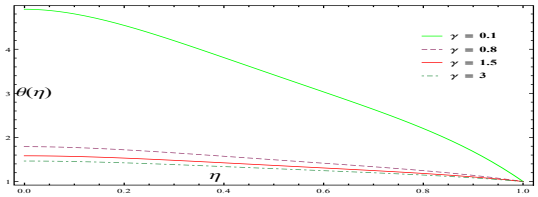

Fig. 20 Variation of the $\theta(\eta)$ with γ, when$R = 1, P_r = 0.5, M = 0.3, \delta = 0.1\ E_c = 0.3$

Table 5 Values of $\theta'(1)$ when $P_r = 0.5, M = 0.3, E_c = 0.1, \delta = 0.1$

		$A = 0.5$		$A = -0.5$	
R	γ	HPM	FDM	HPM	FDM
1	0.3	-0.62097	-0.62065	-6.14852	-6.14594
5		-0.52930	-0.52907	-7.55316	-7.55087
10		-0.46867	-0.46853	-10.12360	-10.12190
15		-0.44496	-0.44445	-13.58400	-13.5850
20		-0.44629	-0.44606	-17.01380	-17.0201
25		-0.46910	-0.46812	-17.2560	-17.2892
-1		-0.68867	-0.68835	-5.62463	-5.62193
-5		-0.89042	-0.88993	-4.85438	-4.85142
-10		-1.34525	-1.34418	-4.27193	-4.26867
-15		-2.21880	-2.2198	-3.96167	-3.95822
-20		-3.90851	-3.90928	-3.81556	-3.81177
-25		-7.19876	-7.20072	-3.76447	-3.76229
1	0.5	-0.43011	-0.429909	-4.25700	-4.25524
5		-0.37105	-0.37087	-5.23339	-5.23189
10		-0.34151	-0.34125	-6.95770	-6.95685
15		-0.34703	-0.34644	-8.75793	-8.76180
20		-0.38714	-0.38634	-7.76800	-7.97814
25		-0.48020	-0.47805	-5.6942	-5.6938
-1		-0.47699	-0.47679	-3.89429	-3.89240
-5		-0.62331	-0.62301	-3.36877	-3.36669
-10		-0.96882	-0.96901	-2.98598	-2.98362
-15		-1.65783	-1.65706	-2.79694	-2.79427
-20		-3.03244	-3.03330	-2.70135	-2.7195
-25		-5.78143	-5.78817	-2.6953	-2.71075

REFERENCES

Abderrahim, W., Zoubair, B., Animasaun, I, L., Afridi, M, I., Qasimd, M., and Rachid, S., 2019, "Magneto-Convection of Alumina Water Nanofluid Within Thin Horizontal Layers Using the Revised Generalized Buongiorno's Model," *Frontiers in Heat and Mass Transfer (FHMT)*, **12**(3), 1–15.
http://dx.doi.org/10.5098/hmt.12.3.

Abderrahim, W., Zoubair, B., Farhad, A., Mohamed, R, E., and Rachid, S., 2018a, "Numerical Analysis of the Unsteady Natural Convection MHD Couette Nanofluid Flow in the Presence of Thermal Radiation Using Single and Two-phase Nanofluid Models for Cu–water Nanofluidsl," *International Journal of Applied and Computational Mathematics*, **4:81**.
https://doi.org/10.1007/s40819-018-0513-y.

Abderrahim, W., Zoubair, B., Mishra, S, R., Mohammad, Mehdi, R., and Rachid, S., 2018b, "Influence of a Uniform Transverse Magnetic Field on the Thermo-Hydrodynamic Stability in Water Based Nanofluids with Metallic Nanoparticles Using the Generalized Buongiorno's Mathematical Model," *The European Physical Journal Plus*, **133:181**.
https://doi.org/10.1140/epjp/i2018-12037-.

Abderrahim, W., Zoubair, B., and Rachid, S., 2017a, "Numerical Analysis of the Onset of Longitudinal Convective Rolls in a Porous Medium Saturated by an Electrically Conducting Nanofluid in the Presence of an External Magnetic Field," *Results in Physics*, **7**, 2134–2152.
https://doi.org/10.1016/j.rinp.2017.06.003.

Abderrahim, W., Zoubair, B., and Rachid, S., 2017b, "Numerical Study of the Onset of Convection in a Newtonian Nanofluid Layer with Spatially Uniform and Non-uniform Internal Heating," *Journal of Nanofluids*, **6**(1), 136–148.
https://doi.org/10.1166/jon.2017.1293.

Abderrahim, W., Zoubair, B., and Rachid, S., 2018c, "A semi-analytical Analysis of Electro-Thermo-Hydrodynamic Stability in Dielectric Nanofluids Using Buongiorno's Mathematical Model Together With More Realistic Boundary Conditions," *Results in Physics*, **9**, 1438–1454.
https://doi.org/10.1016/j.rinp.2018.01.066.

Abdul, M, S., Sania, I., and Ali, R, A., 2008, "Unsteady Squeezing Flow of a Viscous MHD Fluid Between Parallel Plates," *Mathematical Modelling and Analysis*, **13**(4), 565–576.
https://doi.org/10.3846/1392-6292.2008.13.565-576.

Archibald, 1956, "Load Capacity and Time Relations for Squeeze Films," *journal of lubrication technology*, **78**, A231–A245.

Babolian, E., Azizi, A., and Saeidian, 2009, "Some Notes on Using the Homotopy Perturbation Method for Solving Time-Dependent Differential Equations," *Mathematical and Computer Modelling*, **50**(1-2), 213–224.
https://doi.org/10.1016/j.mcm.2009.03.003.

Boulahia, Z., Wakif, A., and Sehaqui, R., 2018, "Heat Transfer and Cu-Water Nanofluid Flow in a Ventilated Cavity having Central Cooling Cylinder and Heated from the Below Considering three Different Outlet Port Locations," *Frontiers in Heat and Mass Transfer*, **11**(11).
http://dx.doi.org/10.5098/hmt.11.11 .

Bujurke, N, M., Achar, P, K., and Pai, N, P., 1995a, "Computer Extended Series for Squeezing Flow Between Plates," *Fluid Dynamics Rese*, **16**(2-3), 173–187.
https://doi.org/10.1016/0169-5983(94)00058-8.

Bujurke, N, M., Pai, N, P., and Achar, P, K., 1995b, "Computer Extended Series Solution to Viscous Flow Between Rotating Discs," *Proceedings Mathematical Sciences*, **1995**(3), 353–369.
https://doi.org/10.1007/BF02837202.

Domairry, G., and Aziz, A., 2009, "Approximate Analysis of MHD Squeeze Flow Between two Parallel Disks with Suction or Injection by Homotopy Perturbation Method," *Mathematical Problems in Engineering*, **2009**, 1–19.
http://dx.doi.org/10.1155/2009/603916.

Grimm, R, J., 1976, "Squeezing Flows of Newtonian Liquid Films an Analysis Include the Fluid Inertia," *Applied Scientific Research*, **32**(2), 149–166.
https://doi.org/10.1007/BF00383711.

Hamza, E, A., 1999, "Suction and Injection Effects on a Similar Flow Between Parallel Plates," *J Phys D: Appl Phys*, **32**(6), 656–663.
https://doi.org/10.1088/0022-3727/32/6/010.

Hayat, T., Abbas, Z., Pop, I., and Asghar, S., 2010, "Effects of Radiation and Magnetic Field on the Mixed Convection Stagnation-Point Flow over a vertical stretching sheet in a porous medium," *International Journal of Heat and Mass Transfer*, **53**(1-3), 466–474.
https://doi.org/10.1016/j.ijheatmasstransfer.2009.09.010.

Hayat, T., Javed, and Abbas, Z., 2008, "Slip Flow and Heat Transfer of a Second Grade Fluid Past a Stretching Sheet Through a Porous Space," *International Journal of Heat and Mass Transfer*, **51**(17-18), 4528–4534.
http://dx.doi.org/10.1155/2009/603916.

Hayat, T., Qasim, M., and Mesloub, S., 2011, "MHD Flow and Heat Transfer Over Permeable Stretching Sheet with Slip Conditions," *International Journal for Numerical Methods in Fluids*, **66**(8), 963–975.
https://doi.org/10.1002/fld.2294.

Hayat, T., Zakir, H., Farooq, M., Alsaedi, A., and Mustafa, O., 2015, "Thermally Stratified Stagnation Point Flow of Casson Fluid with Slip Conditions," *International Journal of Nonlinear Sciences and Numerical Simulation*, **25**(4), 724–748.
https://doi.org/10.1515/ijnsns-2013-0069.

Imran, U., Sharidan, S., and Ilyas, K., 2017, "Effects of Slip Condition and Newtonian Heating on MHD Flow of Casson Fluid over a Nonlinearly Stretching Sheet Saturated in a Porous Medium," *Journal of King Saud University-Science*, **29**(2), 250–259.
https://doi.org/10.1016/j.jksus.2016.05.003.

Jackson, J, D., 1963, "A Study of Squeezing Flow," *Applied Scientific Research, Section A*, **11**(1), 148–152.
https://doi.org/10.1007/BF03184719.

Ji-Huan, H., 2008, "Recent Development of The Homotopy Perturbation Method," *Topol Methods Nonlinear Anal*, **31**(2), 205–209.
https://projecteuclid.org/euclid.tmna/1463150264.

Kuzma, D, C., 1966, "Fluid Inertia Effects in Squeeze Filmsl," *Applied Scientific Research*, **18**(1), 15–20.
https://doi.org/10.1007/BF00382330.

Rajashekhar, C., Manjunatha, G., Vaidya, H., Divya, B., and Prasad, K., 2018, "Peristaltic Flow of Casson Liquid in an Inclined Porous Tube with Convective Boundary Conditions and Variable Liquid Properties," *Frontiers in Heat and Mass Transfer*, **11**(35).
http://dx.doi.org/10.5098/hmt.11.35 .

Reynolds, O., 1886, "On the Theory of Lubrication and its Application to Mr Beauchamp Tower's Experiments, Including an Experimental Determination of the Viscosity of Olive Oil," *Philosophical Transactions of the royal society of London*, **177**, 157–234.
https://doi.org/10.1098/rstl.1886.0005.

Sachdev, P, L., Bujurke, N, M., and Pai, N, P., 2000, "Dirichlet Series Solution of Equations Arising in Boundary Layer Theory," *Mathematical and Computer Modelling*, **32**, 971–980.

Saleem, S., Nadeem, S., Rashid, M, M., and Raju, C, S.K., 2019, "An Optimal Analysis of Radiated Nanomaterial Flow with Viscous Dissipation and Heat Source," *Microsystem Technologies*, **25**(2), 683–689.
https://doi.org/10.1007/s00542-018-3996-x.

Sampath, Kumar, V.S., and Pai, N, P., 2019, "Suction and Injection Effect on Flow Between two Plates with Reference to Casson Fluid Model," *Multidiscipline Modeling in Materials and Structures*, **15**(3), 559–574.
https://doi.org/10.1108/MMMS-05-2018-0092.

Sankad, G., and Patil, A., 2018, "Heat Transfer Inferences on the Herschel Bulkley Fluid Flow Under Peristalsis," *Frontiers in Heat and Mass Transfer*, **10**(17).
http://dx.doi.org/10.5098/hmt.10.17.

Sheikh, I, K., Naveed, A., Umar, K., Saeed, U, J., and Mohyud, S, T., 2015, "Heat Transfer Analysis for Squeezing Flow Between Parallel Disks," *Journal of the Egyptian Mathematical Society*, **23**(2), 445–450.
https://doi.org/10.1016/j.joems.2014.06.011.

Shijun, L., 2011, *Homotopy Analysis Method in Nonlinear Differential Equations*, Springer.

Sobamowo, M, G., and Akinshilo, A, T., 2018, "On The Analysis of Squeezing Flow of Nanofluid Between two Parallel Plates Under the Influence of Magnetic Field," *Alexandria Engineering Journal*, **57**(3), 1413–1423.
https://doi.org/10.1016/j.aej.2017.07.001.

Sufian, M., Ahmer, M., and Asif, A., 2012, "Three-Dimensional Squeezing Flow in a Rotating Channel of Lower Stretching Porous Wall," *Computers and Mathematics with Applications*, **64**(6), 1575–1586.
https://doi.org/10.1016/j.camwa.2012.01.003.

Sumit, G., Devendra, K., and Jagdev, S., 2006, "New Interpretation of Homotopy Perturbation Method," *International Journal of Modern Physics B*, **20**(18), 2561–2568.

Sumit, G., Devendra, K., and Jagdev, S., 2013, "Application of He's Homotopy Perturbation Method for Solving Nonlinear Wave-like Equations with Variable Coefficients," *International Journal of Advances in Applied Mathematics and Mechanics*, **1**(2), 65–79.
http://www.ijaamm.com/uploads/2/1/4/8/21481830/ijaamm-y2013v1n2p6-devendrakumar.pdf.

Tichy, J, A., and Winer, W, O., 1970, "Inertial Considerations in Parallel Circular Squeeze Film Bearings," *Journal of Lubrication Tech*, **92**(4), 588–592.
https://doi.org/10.1115/1.3451480.

Umar, K., Naveed, A., Zaidi, Z, A., Mir, A., and Syed, Tauseef, M.D., 2014, "MHD Squeezing Flow Between two Infinite Plates," *Ain Shams Engineering Journal*, **5**(1), 187–192.
https://doi.org/10.1016/j.asej.2013.09.007.

Umar, K., Sheikh, Irfanullah, K., Naveed, A., Saima, B., and Syed, Tauseef, M.D., 2016, "Heat Transfer Analysis for Squeezing Flow of a Casson Fluid Between Parallel Plates," *Ain Shams Engineering Journal*, **7**(1), 497–504.
https://doi.org/10.1016/j.asej.2015.02.009.